JACS
JOURNAL OF THE AMERICAN CHEMICAL SOCIETY
pubs.acs.org/JACS
Article

H-Bonded Counterion-Directed Enantioselective Au(I) Catalysis

Allegra Franchino, Àlex Martí, and Antonio M. Echavarren*

Cite This: J. Am. Chem. Soc. 2022, 144, 3497−3509
Read Online
ACCESS | Metrics & More | Article Recommendations | Supporting Information

ABSTRACT: A new strategy for enantioselective transition-metal catalysis is presented, wherein a H-bond donor placed on the ligand of a cationic complex allows precise positioning of the chiral counteranion responsible for asymmetric induction. The successful implementation of this paradigm is demonstrated in 5-*exo*-dig and 6-*endo*-dig cyclizations of 1,6-enynes, combining an achiral phosphinourea Au(I) chloride complex with a BINOL-derived phosphoramidate Ag(I) salt and thus allowing the first general use of chiral anions in Au(I)-catalyzed reactions of challenging alkyne substrates. Experiments with modified complexes and anions, ^{1}H NMR titrations, kinetic data, and studies of solvent and nonlinear effects substantiate the key H-bonding interaction at the heart of the catalytic system. This conceptually novel approach, which lies at the intersection of metal catalysis, H-bond organocatalysis, and asymmetric counterion-directed catalysis, provides a blueprint for the development of supramolecularly assembled chiral ligands for metal complexes.

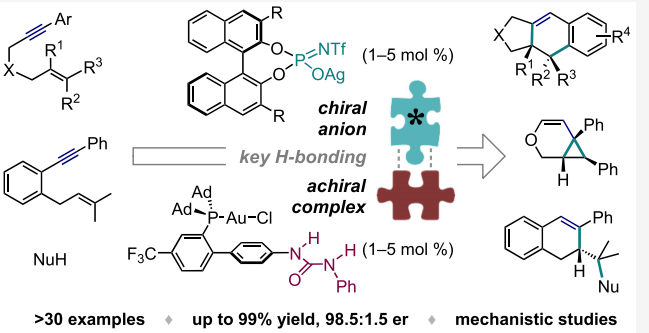

INTRODUCTION

Groundbreaking work by Toste and co-workers proved that it was possible to perform gold catalysis enantioselectively by using achiral ligands together with chiral anions, combining a dinuclear gold complex with a chiral silver phosphate to realize the asymmetric cyclization of allenes (Scheme 1A).[1] This contributed to the development of the field of "asymmetric-counteranion directed catalysis" (ACDC),[2] and chiral anions have since been employed as stereodirecting elements in other Au(I)-catalyzed transformations, in combination with both achiral[3] and chiral[4] gold complexes. However, nearly all examples of Au(I)-ACDC reported to date refer to reactions of prochiral allene substrates.[3,4] The only exceptions are the desymmetrization of diynes described by the group of Czekelius (Scheme 1B)[5] and cases of tandem Au/chiral acid catalysis wherein gold is generally not involved in the enantiodetermining Brønsted acid-catalyzed step.[6] To the best of our knowledge, all other attempts to leverage chiral counterions in more challenging asymmetric Au(I)-catalyzed reactions of alkynes,[7] which, unlike allenes, cannot be prochiral in themselves, were met with failure until now. In this regard, our group reported that mixing triphenylphosphinegold(I) chloride with BINOL-derived silver phosphates affords neutral gold complexes with an anionic phosphate ligand, which are not catalytically competent in enyne cycloisomerizations.[8] In fact, the counteranion has a profound impact on the reactivity and selectivity of all gold-catalyzed transformations, since properties such as its basicity, coordinating ability, and steric bulk influence the energy barriers for various elementary steps of the catalytic cycle.[9,10]

A further layer of complexity is added when the anion is chiral, as its position with respect to the reaction center, key for a successful ACDC, depends on difficult-to-predict electrostatic interactions with the cationic complex/intermediate or on the presence of a protic group on the substrate. Therefore, in the vast majority of cases, the noncovalent interactions required for enantioinduction[11] are not built into the catalytic system *a priori* but rather selected during optimization by a lengthy trial-and-error approach and rationalized only *a posteriori*.[12] Alternatively, the chiral anion can be precisely positioned by a rigid covalent linkage to the ligand, as in the "tethered counterion-directed catalysis" strategy recently disclosed by Marinetti, Guinchard, and co-workers for the enantioselective Au(I)-catalyzed tandem cycloisomerization−nucleophile addition to 2-alkynyl enones.[13] However, despite its elegance, this latter approach becomes akin to using a chiral ligand, so it is devoid of the flexibility and combinatorial potential offered by the original two-component ACDC.

Herein we detail a conceptually novel "H-bonded counterion-directed catalysis" strategy that enables the first general use of chiral anions in gold(I)-catalyzed reactions of alkyne substrates, as opposed to well-established allenes (Scheme 1c). Various bi- and tricyclic structures were accessed in good

Received: November 14, 2021
Published: February 9, 2022

Scheme 1. Asymmetric Counterion-Directed Gold Catalysis

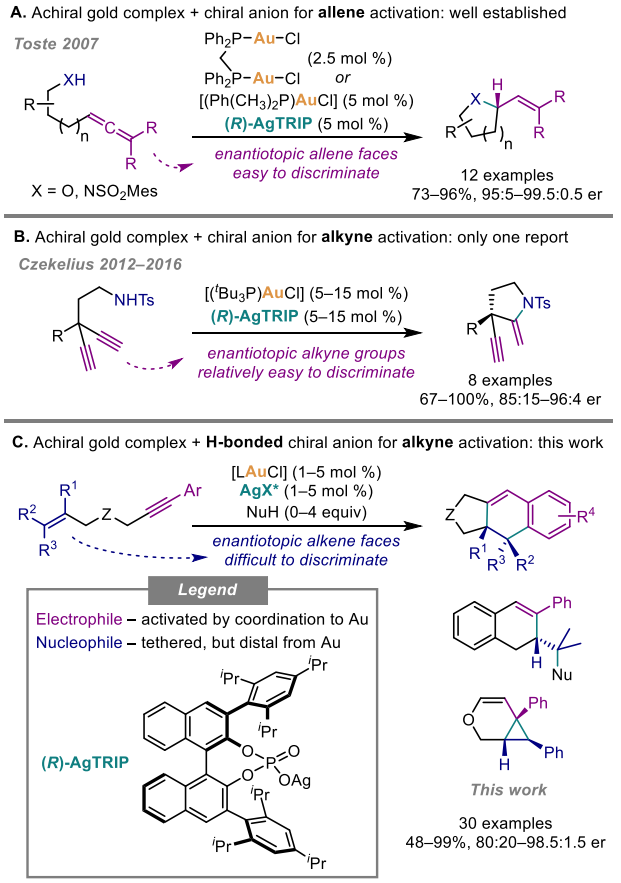

Scheme 2. Design for Asymmetric H-Bonded Counterion-Directed Au(I) Catalysis

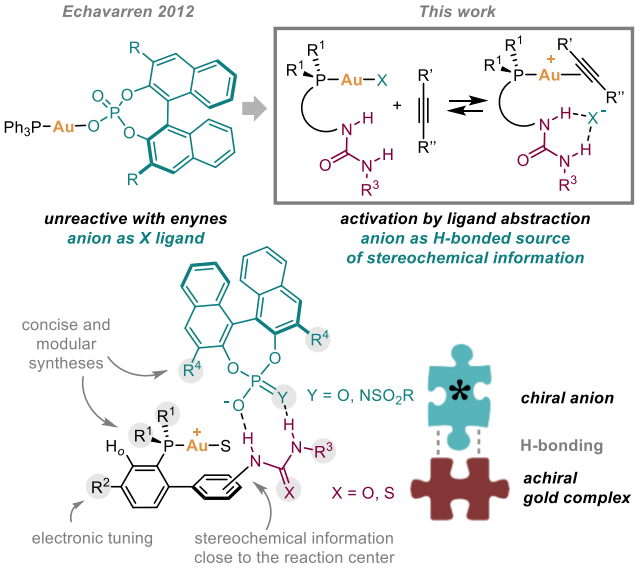

to excellent yield and enantioselectivity from 1,6-enynes, via 5-*exo*-dig and 6-*endo*-dig cyclizations with or without external nucleophiles.[14] To overcome the reactivity[8] and enantiocontrol[15] challenges described above, we envisioned to prepare gold(I) complexes with bifunctional phosphine ligands[16] incorporating dual H-bond donor groups[17] such as (thio)ureas[18] and combine them with BINOL-derived chiral anions[19] (Scheme 2). The pendant H-bond donor would serve two purposes: (1) remove the chiral anionic ligand from the Au(I) coordination sphere, thus enabling substrate coordination and subsequent catalysis at the metal center; (2) place the chiral anion close to the substrate, ensuring good transmission of the stereochemical information.

The feasibility of ligand abstraction via H-bonding interactions was supported by our previous studies on the self-activation of Au(I) chloride complexes featuring PPh_3-based phosphinosquaramides and phosphinoureas.[18b] Regarding stereochemical considerations, we chose Buchwald-type phosphines functionalized at the *meta* or *para* position of the distal aryl ring due to both their easy electronic tuning and attractive geometric features in the context of linear dicoordinated Au(I) complexes (Scheme 2).[16,20] In fact, the blocked rotation about the P−C_{aryl} bond, enforced by the interlocking of the *ortho*-proton H_o between the two bulky alkyl groups, causes the P−Au−Cl and biphenyl axes to be parallel. This in turn projects the urea "anchor" for the chiral anion close to the substrate coordination site. This H-bonded ACDC approach features a modular and easy synthesis for both pieces of the catalytic system, which would click together based on predictable, well-precedented H-bond interactions between (thio)ureas and phosphate anions.[21] This strategy can thus benefit from all the typical advantages offered by *supramolecularly assembled* ligands for enantioselective metal catalysis,[22] most notably (i) simple preparation and tuning of the two components, which avoids long syntheses of new chiral ligands from scratch, and (ii) generation of a large library of catalysts through combinatorial and potentially automated methods, with the aim to speed up screening and optimization.

RESULTS AND DISCUSSION

Synthesis of the Components of the Catalytic System. The bifunctional phosphino(thio)urea Au(I) chloride complexes were prepared with a high-yielding and modular three-step sequence from bromoanilines **A1**−**3**, in turn accessible in one or two steps from commercial building blocks (Scheme 3, see Supporting Information for details). A well-scalable Pd-catalyzed P−C coupling[23] allowed the introduction of different phosphine substituents on the biphenyl scaffold without the need to protect the free amine group. In this sense, the use of potassium phosphate in place of stronger bases such as sodium *tert*-butoxide was instrumental in suppressing undesired Buchwald−Hartwig coupling between the aryl bromide and the NH_2 group. Phosphinoanilines **B1**−**5** were then reacted with the iso(thio)cyanate of choice for the late-stage introduction of the key H-bond donor on ligands **L1**−**13**. Finally, ligand exchange with [(Me_2S)AuCl] afforded Au(I) chloride complexes **Au1**−**13**. Thus, all complexes were prepared in four to five total steps and 42−60% overall yields except for **Au12** featuring an *N*-aryl-*N*′-alkylurea, obtained in 31% overall yield. Previously described complexes **Au14**−**16** with a triarylphosphine backbone were included for comparison.[18b]

Representative complexes were characterized also by single crystal X-ray diffraction (see Supporting Information for a complete overview). In the solid state, all novel phosphinourea Au(I) complexes display an intact Au−Cl bond with the P−Au−Cl axis nearly parallel to the biphenyl axis, as expected. The urea moiety generally adopts an *anti,anti*-conformation (**Au1**, **Au6**, **Au10**, and **Au13**) but displays the much rarer *anti,syn* one[24] in **Au4** and **Au8** and shows various degrees of

https://doi.org/10.1021/jacs.1c11978
J. Am. Chem. Soc. 2022, 144, 3497−3509

Scheme 3. Synthesis of Phosphino(thio)urea Au(I) Chloride Complexes Au1−13[a]

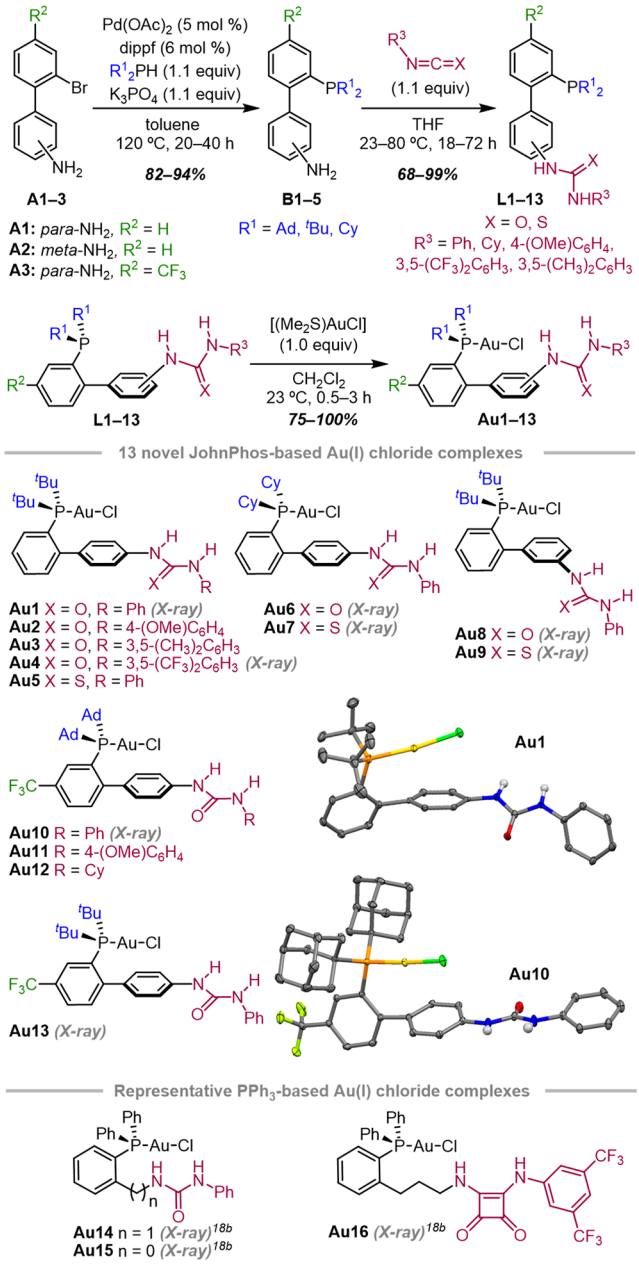

[a]Selected X-ray structures displayed with ORTEP ellipsoid at 50% probability level; solvent molecules and selected H atoms omitted for clarity.

out-of-plane twisting of the aryl substituents (compare **Au1** and **Au10** in Scheme 3). In the solid state, the urea group establishes H-bonds either with chloride ligands or with other urea units, depending on the ligand scaffold. As for phosphinothiourea Au(I) complexes, **Au7** possessing a *para*-substituted ligand shows a classical [LAuCl] structure with intramolecular NH···Cl contacts. In the crystal structure of **Au9**, on the contrary, the S atom of the *meta* thiourea coordinates to gold with an almost linear P−Au−S axis, while the displaced chloride ion is stabilized by two H-bonds with the NH groups.

Regarding the other component of the catalytic system, we planned to introduce the chiral anion as a metal salt in order to simultaneously scavenge the chloride ligand from the Au(I) center. To this end, eight chiral salts (**Ag1−6**, **Na6**, and **Cu6**) were synthesized in 2−3 steps and 30−77% overall yield from commercially available (*R*)-configured binaphthols **C1−4** (Scheme 4). After treatment of the latter with phosphoryl

Scheme 4. Synthesis of Ag(I), Na(I), and Cu(II) Chiral Salts[a]

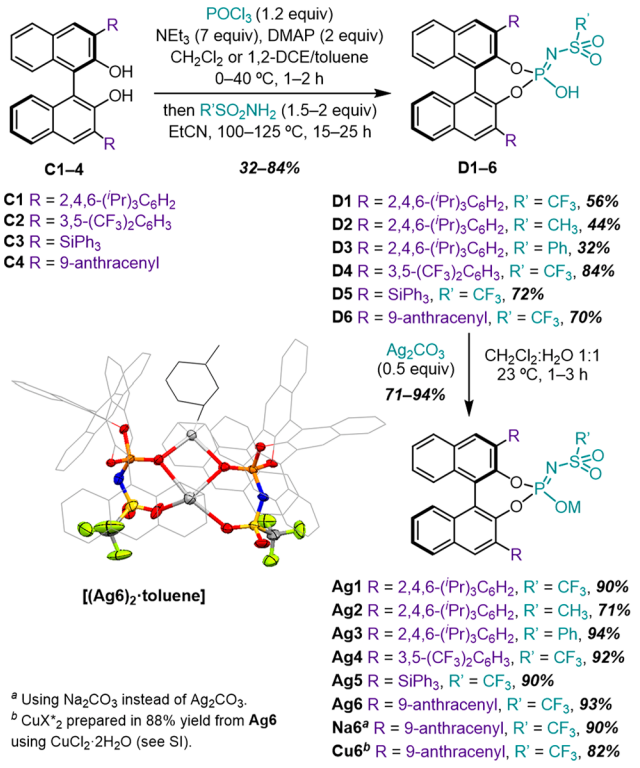

[a]X-ray structure displayed with ORTEP ellipsoid at 50% probability level; binaphthol scaffold and toluene in wireframe; selected solvent molecules and all H atoms omitted for clarity.

chloride, the desired sulfonamide was added to the reaction mixture affording phosphoramidates[25] **D1−6**. Deprotonation of these Brønsted acids with silver carbonate delivered chiral silver salts **Ag1−6**. Crystals of **Ag6** grown in toluene/pentane reveal a dimeric structure where the anion behaves as a bidentate *O*,*O*-ligand through the phosphoryl and sulfonyl O atoms (Scheme 4). The Ag(I) centers are further stabilized by η^2-interactions with the anthracenyl substituents, and one of them is also bound in a η^1/η^2 fashion to a molecule of toluene.

Optimization. Having built the library of [LAuCl] complexes and chiral anions, to validate our H-bonded ACDC design, we investigated the cycloisomerization of 1,6-enynes of type **1** (Table 1),[26,27] a reaction that did not proceed at all employing [(Ph$_3$P)Au(TRIP)].[8] We commenced by screening different silver salts in combination with phosphinourea gold(I) chloride **Au1** at room temperature. This complex combined with **AgTRIP** was catalytically inactive, whereas together with less basic *N*-triflyl phosphoramidate[25] salt **Ag1** afforded the desired product **2a** in good yield and encouraging 79:21 er (Table 1, entries 1 and 2). The more basic *N*-mesyl and *N*-phenylsulfonyl analogues **Ag2** and **Ag3** induced comparable enantioselectivity but much lower reactivity (Table 1, entries 3 and 4). A clear trend between reactivity and basicity emerged: less basic counterions from

https://doi.org/10.1021/jacs.1c11978
J. Am. Chem. Soc. 2022, 144, 3497−3509

Table 1. Screening of Silver Salts with Au1

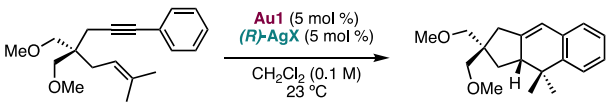

1a (0.05 mmol) 2a

entry	(R)-AgX	time (h)	yield (%)[a]	er[b]
1	**AgTRIP**	96	<5	
2	**Ag1**	4.5	70	79:21
3	**Ag2**	4.5	7	81.5:18.5
4	**Ag3**	4.5	9	83.5:16.5
5	**Ag4**	4.5	42	57:43
6	**Ag5**	4.5	22	51:49

[a]Determined by ^{1}H NMR against internal standard. [b]Determined by HPLC on chiral stationary phase.

stronger parent Brønsted acids[19,28] are essential for reactivity presumably because they coordinate less strongly to the cationic Au(I) center (which is isolobal to a proton)[29] and therefore can be abstracted more easily via H-bonds. Among *N*-triflyl phosphoramidate salts, **Ag1** provided better enantiocontrol than **Ag4** and **Ag5** (Table 1, entries 5 and 6), which bear different groups at the 3,3′-positions of the binaphthol backbone. Overall, the results summarized in Table 1 indicate that for a given anion, substitution at phosphorus influences basicity and coordinating ability, hence reactivity, while 3,3′ residues are responsible for enantioselectivity, as expected.[30]

Next, the library of gold complexes was evaluated with the optimal silver salt (*R*)-**Ag1**. Only key data providing insight into the working mode of the catalytic system are shown in Table 2 (see Supporting Information for comprehensive

Table 2. Screening of Selected Au(I) Complexes with Ag1

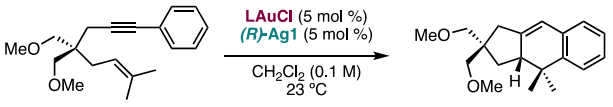

1a (0.05 mmol) 2a

entry	LAuCl	time (h)	yield (%)[a]	er[b]
1	**Au1**	4.5	70	79:21
2	[(JohnPhos)AuCl]	6	40	50:50
3	**Au5**	44	0	
4	**Au8**	4.5	70	27.5:72.5
5	**Au14**	44	32	50:50
6	**Au15**	44	10	45:55
7	**Au16**	24	46	56:44
8[c]	**Au1**	0.7	90	87:13

[a]Determined by ^{1}H NMR against internal standard. [b]Determined by HPLC on chiral stationary phase. [c]In benzene.

optimization studies). The presence of the urea group on the ligand is important for reactivity and essential for enantioselectivity, as [(JohnPhos)AuCl] with **Ag1** delivered product **2a** in lower yield and racemic form (Table 2, entries 1 and 2). Complex **Au5**, the thiourea analogue of **Au1**, was completely inactive, most likely because the S atom of the thiourea coordinates too strongly to the metal center, preventing substrate activation. This is consistent with the known thiophilicity of gold,[31] the Au−S bond observed in the crystal structure of related **Au9**, and previous studies on PPh_3-based phosphinothourea Au(I) complexes.[18b] Moving the urea group from the *para* to the *meta* position of the biphenyl scaffold reversed the sense of enantioinduction (Table 2, entry 4 vs 1). Remarkably, either enantiomer of the product can thus be obtained preferentially using the same enantiomer of the chiral anion, in combination with a different achiral cocatalyst. Complexes **Au14**−**16**, equipped with urea or squaramide groups on triarylphosphine scaffolds,[18b] were poorly active and afforded (almost) racemic product (Table 2, entries 5−7).

This data set highlights that a H-bond donor on the ligand is crucial for both reactivity and enantiocontrol. The mere presence of a chiral anion in the reaction mixture is not sufficient to transfer effectively the stereochemical information, as its proximity to the reaction center cannot be guaranteed in the absence of a suitably placed H-bond donor. These observations lend credibility to the original design, wherein the pendant urea was envisioned to enable both anion abstraction and precise positioning of the source of chirality (Scheme 2). The presence of H-bonding at the heart of the catalytic system can be inferred also from solvent effects. For instance, the performance of the optimal **Au1**/**Ag1** combination improved by replacing dichloromethane with benzene (Table 2, entry 1 vs 8, 79:21 vs 87:13 er). The enantiocontrol generally increased at −20 °C (Table 3). A qualitative

Table 3. Solvent Effect with Au1/Ag1 Catalytic System[a]

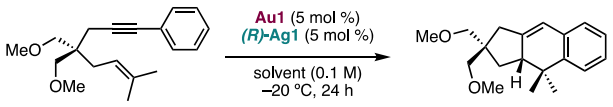

1a (0.05 mmol) 2a

entry	solvent	E^N_T (ref 32)	yield (%)[a]	er[b]
1	$CHCl_3$	0.259	39	93:7
2	CH_2Cl_2	0.309	85	92:8
3	$ClCH_2CH_2Cl$	0.327	60	88:12
4	$C_6H_5CH_3$	0.099	>95	94.5:5.5
5	$1,2\text{-}(CH_3)_2C_6H_4$	na	86	93:7
6	C_6H_5Cl	0.188	>95	91:9
7	C_6H_5F	0.194	75	90:10
8	$C_6H_5CF_3$	na	89	90.5:9.5

[a]Determined by ^{1}H NMR against internal standard. [b]Determined by HPLC on chiral stationary phase.

correlation between solvent polarity (defined by E^N_T values)[32] and enantioselectivity levels was observed, in agreement with H-bonding interactions between the urea and the anion being favored in apolar solvents. The least polar solvent for either the chlorinated or aromatic series (chloroform for entries 1−3 and toluene for entries 4−8 in Table 3) delivered the product with the highest enantiomeric ratio, up to 94.5:5.5 er.

Once identified toluene as the best solvent, a final fine-tuning of the catalytic system was performed (Table 4). Replacing **Ag1** with **Ag6**, i.e., swapping the triisopropylphenyl groups for 9-anthracenyl substituents at the 3,3′-binaphthol positions, led to a considerable improvement in enantioselectivity, although at the expense of conversion (Table 4, entries 1 and 2). In order to increase reactivity, more electrophilic Au(I) complex **Au10** with a trifluoromethyl group *meta* to the phosphine was employed, and an excellent yield of **2a** could be obtained at −10 °C while maintaining the high enantioselectivity (Table 4, entries 3 and 4). Complexes **Au2**−**4**, **Au11**, and **Au12** with different substituents on the urea were also evaluated, since electronic properties influence H-bonding ability.[17,21] However, none of them surpassed the

https://doi.org/10.1021/jacs.1c11978
J. Am. Chem. Soc. 2022, 144, 3497−3509

Table 4. Fine Tuning of the Catalytic System[a]

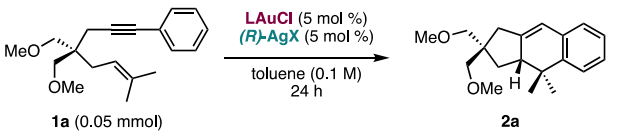

1a (0.05 mmol) 2a

entry	LAuCl	(*R*)-AgX	*T* (°C)	yield (%)[a]	er[b]
1	**Au1**	**Ag1**	−20	>95	94.5:5.5
2	**Au1**	**Ag6**	−20	50	98:2
3	**Au10**	**Ag6**	−20	78	98:2
4	**Au10**	**Ag6**	−10	>95	98:2

[a]Determined by ^{1}H NMR against internal standard. [b]Determined by HPLC on chiral stationary phase.

performance of complex **Au10** possessing a simple phenyl urea, which offered the right balance between electronic activation and steric hindrance (see Supporting Information for details).

Generality of the Enantioselective 5-*exo*-dig and 6-*exo*-dig Cyclizations. The substrate scope of the formal [4 + 2] cycloaddition of enynes **1** catalyzed by the **Au10**/**Ag6** system was then assessed (Scheme 5). Enynes **1a**−**h** bearing various linkers underwent cyclization to deliver the corresponding products **2a**−**h** in high yield (84−95%) and with excellent enantioselectivity (96:4 to 98:2 er). The standard reaction to **2a** could be performed on 2-mmol scale in 24 h under air and in technical-grade toluene, with Au(I) and Ag(I) loading reduced to 1 mol %, with a 99% yield and 98:2 er for the product. This catalyst loading is the lowest reported so far in asymmetric cycloisomerizations of enynes **1**, which is remarkable considering that all previous methods relied on stereochemical information covalently embedded in a chiral ligand.[27] Apart from ethers (**2a**, **2b**), also allyl (**2c**), ester (**2d**, **2h**), carbamate (**2e**), tosylate (**2f**), and acetal groups (**2g**) were tolerated. As for variations on the alkyne moiety, products with electron-poor as well as electron-rich groups at the *para* (**2i**−**l**), *ortho* (**2m**,**n**), and *meta* position (**2o**,**p**) of the aromatic ring were obtained with good to excellent yield and enantiocontrol (85−98%, 89.5:10.5 to 98.5:1.5 er). Also substrates **1q** and **1r**, possessing respectively 1-naphthyl and benzothiophenyl substituents at the alkyne terminus, underwent reaction smoothly and enantioselectively. The attainment of such high levels of enantiocontrol across a broad scope is unprecedented in this transformation.[27]

Compared to linker and alkyne variations, the catalytic system showed higher sensitivity to changes to the alkene part (compare **2a** with **2s**−**w** in Scheme 5), in line with the fact that the chiral catalytic ensemble needs to discriminate the two enantiotopic faces of the double bond. Thus, enynes **1s** and **1t** possessing geranyl or *trans*-cinnamyl groups cyclized to products **2s** and **2t** in less than 48 h (90−99% yield, 89:11 to 95.5:4.5 er), even though higher temperatures and/or catalyst loadings were required. Nevertheless, this marks a significant improvement with respect to previous chiral gold catalysts, which required 7−14 days at room temperature.[27e] Enyne **1u** possessing a *cis*-cinnamyl substituent afforded product **2u** in lower yield (48%, due to a competing cycloisomerization to an achiral diene product) and enantioselectivity (82:18 er). Formation of epimeric products **2t** and **2u** highlights the stereospecificity of the reaction with respect to the alkene configuration. More hindered substrates such as **1v** and **1w**, bearing respectively a cyclohexene or a tetrasubstituted alkene, delivered products **2v** and **2w** in good

Scheme 5. Enantioselective Formal [4 + 2] Cycloadditions of 1,6-Enynes Based on 5-*exo*-dig Cyclizations[a]

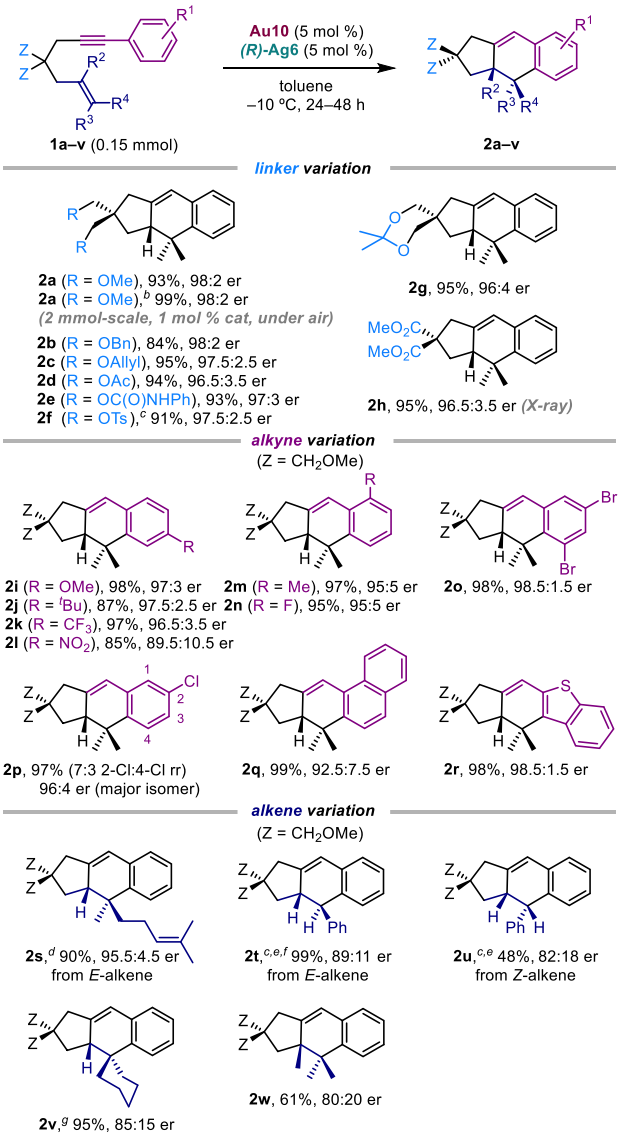

[a]Reactions performed under Ar or N_2 in anhydrous toluene (0.1 or 0.2 M), unless otherwise stated. Yields of material isolated after purification, er determined by HPLC or SFC on chiral stationary phase. [b]Carried out at 2 mmol scale, with 1 mol % **Au10** and 1 mol % **Ag6**, in technical-grade toluene (0.6 M) under air for 24 h. [c]At 23 °C. [d]At 0 °C. [e]With 10 mol % **Au10** and 10 mol % **Ag6**. [f]Including 5% of inseparable 6-*endo*-isomer. [g]Reaction time: 96 h.

yield (61−95%) and moderate but encouraging enantioselectivity (80:20 to 85:15 er), considering that such bulky enynes were never engaged in this cycloisomerization, let alone asymmetrically.

Judging by the enantioselectivity of the 5-*exo*-dig cyclizations presented in Scheme 5, the key interaction between the urea and the anion is not disrupted by H-bond acceptors on the substrates (such as ester, carbamate, tosylate, and nitro groups in **1d**−**f**, **1h**, **1l**), even though they are present in up to 40-fold excess with respect to the chiral anion. Protic additives with H-bond donor ability were also tolerated, as spiking the reaction of model enyne **1a** with 5 equiv of methanol still delivered product **2a** in 80% NMR yield and 97:3 er. These observations suggest that H-bonding between the urea and the anion is

https://doi.org/10.1021/jacs.1c11978
J. Am. Chem. Soc. 2022, 144, 3497−3509

strong enough to make for an effective and robust catalytic system, even if based on noncovalent interactions. To further prove this point, the **Au10**/**Ag6** catalytic system was applied also to the 6-*endo*-dig cyclization of enynes, with and without the addition of protic exogenous nucleophiles (Scheme 6).

Scheme 6. Enantioselective 6-*endo*-dig Cyclizations of 1,6-Enynes without (A) or with (B) Nucleophile Addition[a]

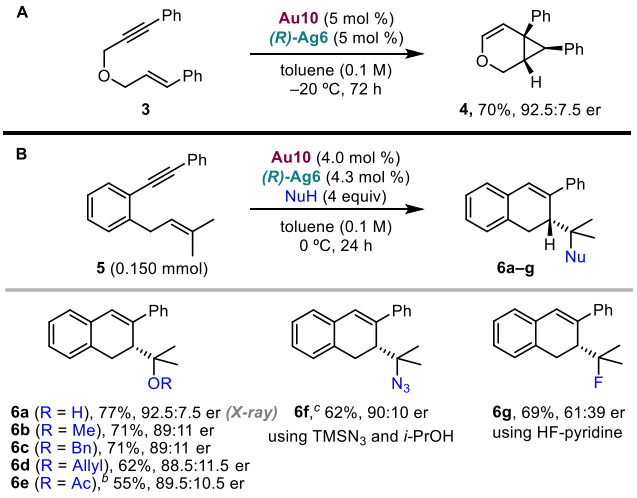

[a]Yields of material isolated after purification, er determined by HPLC or SFC on chiral stationary phase. [b]For 48 h. [c]At 23 °C.

Thus, O-tethered enyne **3** was converted to oxabicyclo[4.1.0]hept-4-ene **4** in 70% yield and 92.5:7.5 er.[33] Cyclization of benzene-tethered enyne **5** followed by the addition of O-based nucleophiles[27e,34] delivered compounds **6a**–**e** in moderate to good yield and er (55–77%, 88.5:11.5 to 92.5:7.5 er).[35] The addition of a N-centered nucleophile to enynes of type **5** was demonstrated for the first time, obtaining azide **6f** in 62% yield and 90:10 er. Instead, fluoride addition afforded product **6g** in 69% yield and only 61:39 er. The low enantiocontrol in the formation of **6g** can be explained by the strong tendency of the fluoride ion to H-bond with the urea,[36] thus preventing the key interaction that keeps the chiral anion in place.

Importantly, derivatization of the water- and azide-addition products gave access to O- and N-derivatives equivalent to the formal addition of noncompetent nucleophiles, thus expanding the scope and underlying the usefulness of this enantioselective protocol. For example, alcohol **6a** was transformed into benzoate **6h**, as well as into diene **7**, which displays the core of the carexane natural products (Scheme 7A).[27e,37] Triazole **6i**, primary amine **6j**, and amide **6k** were easily obtained from azide **6f** without erosion of the enantiopurity (Scheme 7B). Cyclizations of 1,6-enynes bearing a terminal alkyne generally proceeded with lower enantioselectivity than those of internal aryl alkyne substrates (Scheme 7C). The methoxycyclization of benzene-tethered enyne **8** delivered product **9** in 94% yield and 78.5:21.5 er, which could be increased to 87:13 er at the expense of yield (see Supporting Information for details).[38] In order to preserve the stereocenter, the cyclopropyl gold carbene generated upon 5-*exo*-dig cycloisomerization of O-tethered enyne **10** was trapped *in situ* with diphenyl sulfoxide.[39] Under unoptimized conditions, cyclopropyl aldehyde **11** was obtained in 42% yield and 83:17 er, which

Scheme 7. Derivatization and Scope Extension

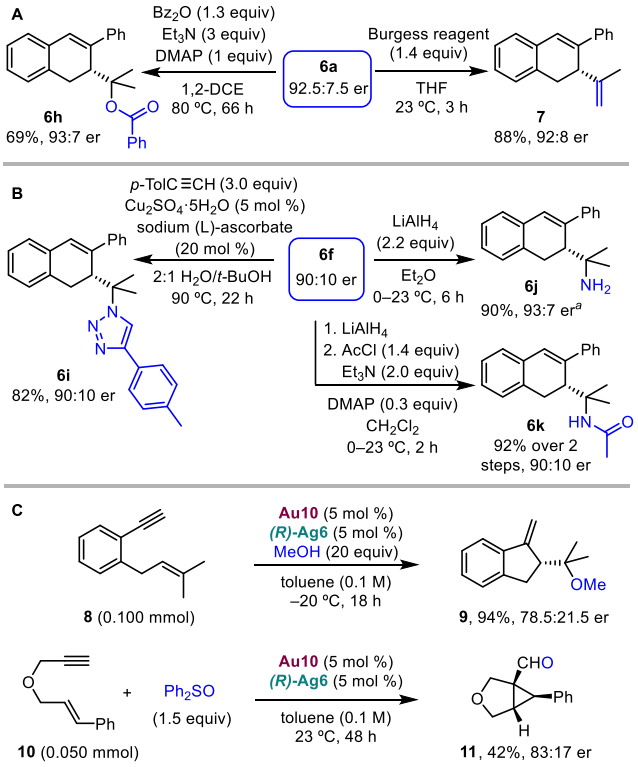

[a]Prepared from a batch of **6f** with 93:7 er (see Supporting Information).

compares favorably with the only other enantioselective preparation reported so far (3% ee).[40]

Finally, we sought to extend this H-bonded counterion-directed catalysis strategy to other types of reactions. At 1 mol % loading, phosphinosquaramide complex **Au16** in combination with (*R*)-**Ag6** catalyzes the tandem cyclization–indole addition to 2-alkynyl enones **12**, affording furans **14a**–**d** in good yield and enantioselectivity (Scheme 8).[41,13] In this case,

Scheme 8. Enantioselective Cycloisomerization–Indole Addition to 2-Alkynyl Enones[a]

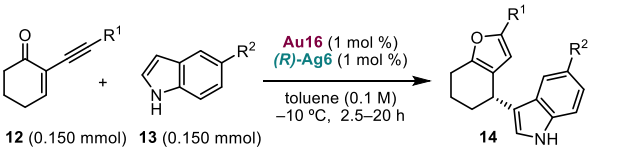

[a]Yields of material isolated after purification, er determined by HPLC or SFC on chiral stationary phase.

the stereocenter is not created during the cycloisomerization but forms in the subsequent intermolecular nucleophilic attack to a carbocation intermediate. Chiral salt (*R*)-**Ag6** alone affords predominantly the opposite enantiomer of product **14a**, and the **Au10**/(*R*)-**Ag6** combination employed for 1,6-enynes gives slightly lower enantioselectivity. These results indicate that tuning of the *achiral* catalytic component to get high enantioselectivity is required for each reaction class (see

https://doi.org/10.1021/jacs.1c11978
J. Am. Chem. Soc. 2022, 144, 3497–3509

Supporting Information for more examples, including an allenol[1] cyclization).

Mechanistic Studies. Additional control experiments were conducted to shed light on the working mode of the final, optimized **Au10**/**Ag6** catalytic system (Scheme 9 and Table 5, see Supporting Information for further tests). To this end, cationic complex **Au17** was prepared by treatment of **Au10** with equimolar $AgSbF_6$ in the presence of acetonitrile. Its structure was confirmed by X-ray diffraction, showing that in the solid state the urea H-bonds to the fluoride of the counteranion. When $AgSbF_6$ was replaced by (*R*)-**Ag6**, neutral complex **Au18** was isolated instead, with no incorporation of acetonitrile as indicated by NMR.

Scheme 9. Synthesis of Complexes with Ureaphosphine L10

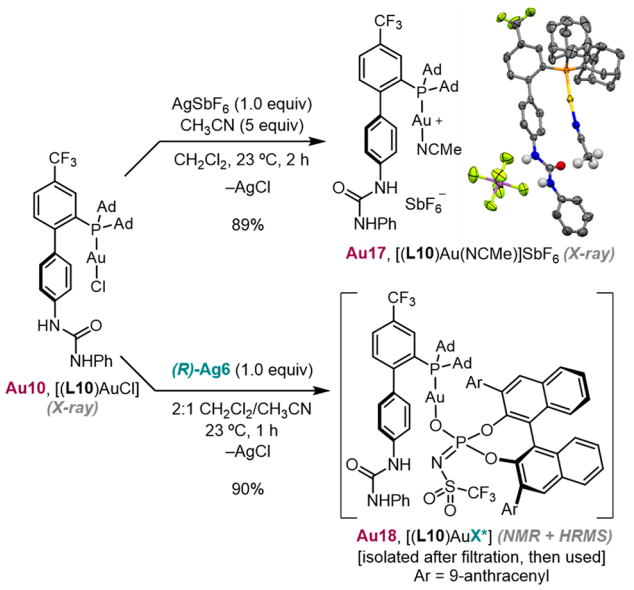

These complexes were then used in a series of informative control experiments, which highlighted how the chloride ligand and the countercation of the chiral salt play a role too (Table 5). Preformed complex **Au18** delivered product **2a** with yield and enantioselectivity comparable to the *in situ* combination of **Au10** and (*R*)-**Ag6** (93:7 er vs 98:2 er, Table 5, entries 1 and 2). No reactivity was detected employing either [(JohnPhos)AuCl] with (*R*)-**Ag6** or **Au10** with (*R*)-**Na6** (Table 5, entries 3 and 4), indicating respectively that the urea is required to remove the chiral anion from Au and that sodium, unlike silver, is not able to scavenge the chloride ligand. Experiments with cationic complexes **Au17** and its urea-free counterpart [(JohnPhos)Au(NCMe)]SbF_6 were then performed. Combining [(JohnPhos)Au(NCMe)]SbF_6 with (*R*)-**Ag6** and (*R*)-**Na6** delivered racemic material in low yield (Table 5, entries 5 and 6), thus emphasizing the importance of the tethered urea not only for reactivity but also for enantioselectivity, achieved through precise positioning of the chiral anion via H-bonding. In an apparently surprising outcome, also cationic complex **Au17** combined with (*R*)-**Ag6** yielded racemic product (Table 5, entry 7). This can actually be explained by catalysis carried out by achiral cationic species **Au17** on its own, because the chiral anion associates preferentially to Ag^+ over Au^+ (or the urea). In agreement with this picture, product **2a** was obtained with 79:21 er when (*R*)-**Na6** was used (Table 5, entry 8). Moreover, when 1 equiv of 15-crown-5 ether was added in order to chelate Na^+ and thus direct the anion to Au^+, the enantiomeric ratio of the product further improved to 90:10 (Table 5, entry 9). Therefore, in order to attain high enantioselectivity using this H-bonded system, it is crucial to tie the generation of the catalytically competent cationic Au(I) center to the removal of other cations (Ag^+ and to a lesser extent Na^+), which would otherwise "sequester" the chiral anion, leading to racemic background reactivity. In this sense, when combining **Au10** and (*R*)-**Ag6** *in situ*, precipitation of AgCl not only frees up a coordination site on gold but also ensures that Ag^+ is removed from deleterious solution equilibria with the anion.

Further insights into the catalytic system are presented in Scheme 10. First of all, single-crystal X-ray diffraction of products **2h** and **6a** and comparison of optical rotations with available literature values indicate that the newly created stereocenter is (*R*)-configured in both 5-*exo*-dig and 6-*endo*-dig reactions. This implies that in the enantiodetermining step of both cyclization modes, the *Si* face of the alkene attacks the Au(I)-activated alkyne, delivering the corresponding cyclopropyl Au(I) carbene intermediates (Scheme 10A). The absence of nonlinear effects (Scheme 10B) suggests that only one chiral anion is involved in the enantiodetermining step, in line with formation of the expected 1:1 urea:anion complex.[21b,c]

Table 5. Control Experiments

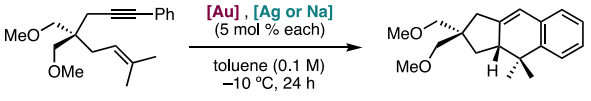

entry	[Au]	[Na or Ag]	yield (%)[a]	er[b]
1	**Au10**	(*R*)-**Ag6**	>95	98:2
2	**Au18**		>95	93:7
3	[(JohnPhos)AuCl]	(*R*)-**Ag6**	0	
4	**Au10**	(*R*)-**Na6**	0	
5	[(JohnPhos)Au(NCMe)]SbF_6	(*R*)-**Ag6**	24	50:50
6	[(JohnPhos)Au(NCMe)]SbF_6	(*R*)-**Na6**	3	50:50
7	**Au17**	(*R*)-**Ag6**	>95	50:50
8	**Au17**	(*R*)-**Na6**	>95	79:21
9[c]	**Au17**	(*R*)-**Na6**	>95	90:10

[a]Determined by ^{1}H NMR against internal standard. [b]Determined by HPLC on chiral stationary phase. [c]With 15-crown-5 (100 mol %).

https://doi.org/10.1021/jacs.1c11978
J. Am. Chem. Soc. 2022, 144, 3497−3509

Scheme 10. Mechanistic Investigations: (A) Enantiofacial Selectivity, (B) Study of Nonlinear Effects, (C) Use of Complex Au4 as Au10 Surrogate, (D) ^{1}H NMR Titration of Au4 with (*R*)-Na6 (298 K, CD_2Cl_2), (E–J) Kinetic Studies

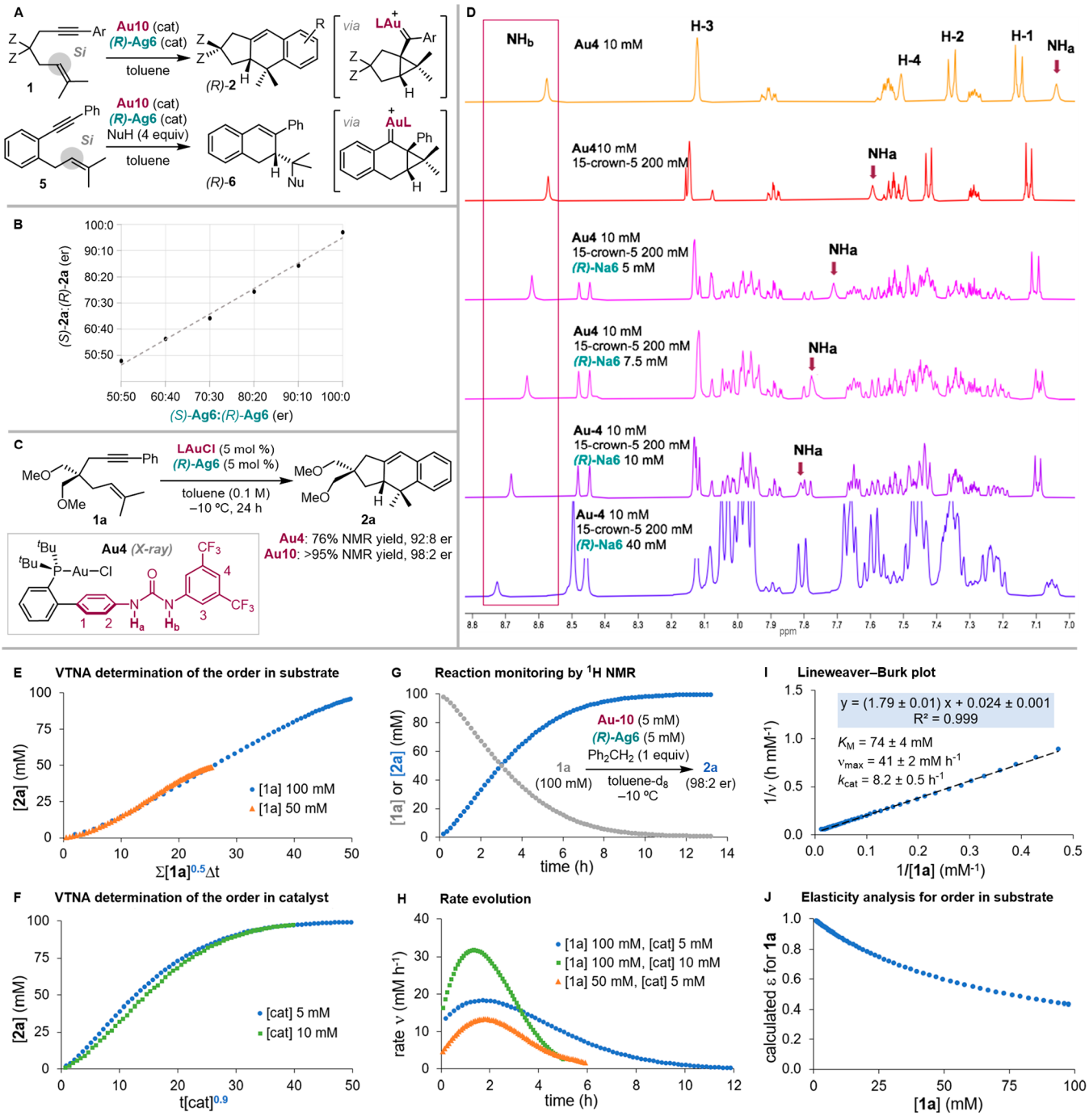

Spectroscopic observation of the H-bonding interaction between the urea of complex **Au10** and the chiral anion proved to be nontrivial. Mixing of **Au10** and (*R*)-**Ag6**, in various ratios and in the absence of substrate, invariably resulted in at least partial chloride abstraction. In turn this led to poorly resolved NMR spectra, where species tentatively identified as chiral [LAuX] **Au18** with the anion behaving as anionic ligand, and achiral chloride-bridged dinuclear complexes predominated. On the other hand, when **Na6** was used instead of **Ag6** to circumvent chloride scavenging, no changes were detected by NMR. In this last case, the chiral anion presumably remained associated with Na^+ without interacting at all with the neutral urea. We resorted to study the combination of (*R*)-**Na6** and complex **Au4** in the presence of a constant excess of 15-crown-5, to force dissociation of the sodium cation, while at the same time avoiding undesired chloride scavenging. Au(I) chloride complex **Au4** was chosen as a convenient surrogate for **Au10**, since the NH signals of its bis(trifluoromethyl)phenylurea resonate in a free region of the ^{1}H NMR spectrum. The performance of **Au4** in the standard asymmetric reaction is comparable to that of **Au10**, even if with marginally lower reactivity (consistent with the absence of the *meta* CF_3 group) and enantioselectivity (Scheme 10C). Gratifyingly, ^{1}H NMR titration of complex **Au4** (10 mM in CD_2Cl_2 at 25 °C) with

https://doi.org/10.1021/jacs.1c11978
J. Am. Chem. Soc. 2022, 144, 3497–3509

Scheme 11. Proposed Mechanism for the Cyclization of Enyne 1 under H-Bonded Counterion-Directed Au(I) Catalysis

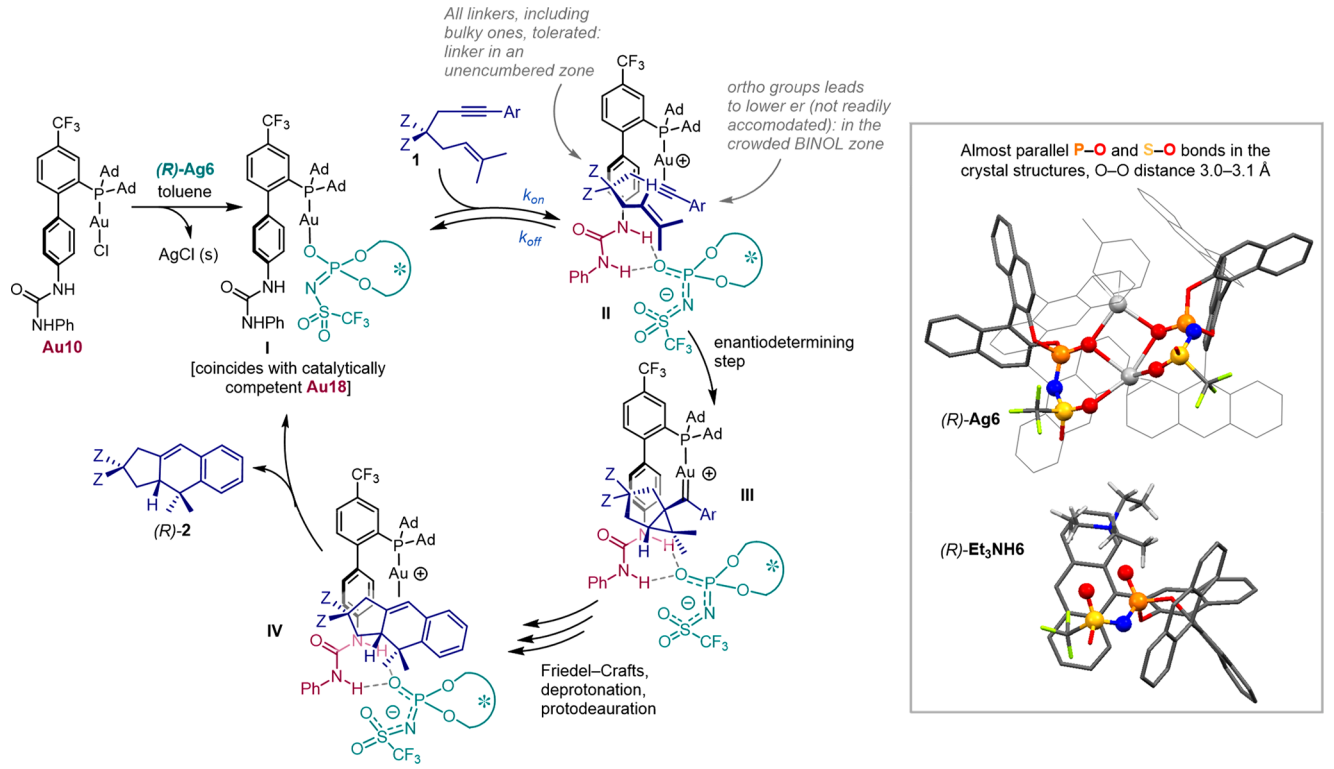

increasing amounts of (*R*)-**Na6** in the presence of 20 equiv of 15-crown-5 resulted in clear deshielding of both NH signals of the urea, indicating their engagement in H-bonds with the anion (Scheme 10D).[42] The titration was recorded at the same catalyst concentration present in the reaction mixtures (5−10 mM), and the establishment of such H-bonds during the reaction is expected to be entropically even more facile because after AgCl precipitation the Au(I)-bound chiral anion should already be in close proximity to the H-bond donor.

Finally, kinetic studies on the cycloisomerization of **1a** to **2a** catalyzed by the **Au10**/(*R*)-**Ag6** system in toluene-d_8 at −10 °C were undertaken. By use of the variable time normalization analysis (VTNA) introduced by Burés,[43] the reaction was found to be approximately first order in catalyst (0.9) and 0.5 order in substrate (Scheme 10E,F). A first order in catalyst is common to most catalyzed transformations, provided that the catalyst does not decompose or aggregate into off-cycle species. A partial, noninteger order in substrate is expected for unimolecular catalyzed reactions that follow Briggs−Haldane kinetics[44] and possess a Michaelis−Menten constant[45] (K_M) similar to substrate concentration.[18b] To verify that this was indeed the case for the cycloisomerization under study, the reaction progress kinetic analysis (RPKA) popularized by Blackmond[46] was carried out. ^{1}H NMR monitoring of the reaction indicated clean conversion of enyne **1a** to product **2a** (Scheme 10G), but rate analysis revealed an initial induction period (Scheme 10H), most likely related to a noninstantaneous chloride abstraction.[47] The double reciprocal Lineweaver−Burk plot was thus constructed using data in the 1.5−10 h time range (Scheme 10I),[48] obtaining a Michaelis−Menten constant (K_M) of 74 ± 4 mM.[49] Given the 0−100 mM substrate concentration present during the reaction, this intermediate K_M value justifies the partial order in substrate determined by VTNA. The experimental 0.5 order found for the entire reaction course falls within the range of the calculated elasticity coefficient ε,[50] which predicts the changing order in substrate for Briggs−Haldane kinetic regimes from K_M and substrate concentration (Scheme 10J).

Scheme 11 presents a tentative mechanism for the enantioselective formal [4 + 2] cycloaddition of enyne **1a** catalyzed by **Au10**/(*R*)-**Ag6**, which takes into account all the experimental, spectroscopic, and kinetic evidence discussed above, as well as previous studies on this cycloisomerization.[26b,27e] Upon mixing Au(I) chloride complex **Au10** with (*R*)-**Ag6**, neutral complex **I** possessing a phosphoramidate anionic ligand forms. The expected chloride scavenging accompanied by precipitation of AgCl matches the observed formation of a solution (with very few solid grains) upon addition of a solution of (*R*)-**Ag6** to a thick whitish suspension of **Au10** and enyne in toluene. Species **I** represents the entry to the catalytic cycle and coincides with **Au18**, prepared *ex situ* (see Scheme 9) and catalytically competent (see Table 5). In the presence of enyne **1**, neutral complex **I** is proposed to be in equilibrium with cationic complex **II**, wherein the anion is H-bonded to the pendant urea and the alkyne coordinates to Au. The presence of this equilibrium is consistent with the partial order in substrate observed in the Briggs−Haldane kinetics. Additionally, H-bonding interactions between the anion and both NH groups of the urea were observed spectroscopically in a model system (see Scheme 10D). Regarding their precise geometrical arrangement, we propose that the NH residues establish two H-bonds with the phosphoryl O atom. This speculation is based on solid state considerations and DFT calculations with implicit solvent models.[51] In the crystal structures of (*R*)-**Ag6** and related triethylammonium salt (*R*)-**Et$_3$NH6**, the P−O and S−O bonds are almost parallel with the two O atoms forming a ∼3 Å wide "pincer" (see inset in

https://doi.org/10.1021/jacs.1c11978
J. Am. Chem. Soc. 2022, 144, 3497−3509

Scheme 11), while **Au10** has a 2.0 Å H−H distance between the urea NH groups. The most stable conformer computed by DFT for the model diphenylurea−chiral phosphoramidate couple shows two H-bonds to the phosphoryl O atom; however, a conformer where the NH groups H-bond to both the phosphoryl and sulfonyl O atoms is only 0.8 kcal/mol higher in energy.[51]

The enyne is expected to be oriented as depicted for complex **II** (Scheme 11), with the arene pointing toward the more crowded BINOL region and the linker in an unencumbered zone. This would be consistent with the lower er (92.5:7.5 to 95:5) observed in the cyclization of *ortho*-substituted substrates **1m**, **1n**, and **1q**, which are not so well accommodated, and with the catalyst ability to tolerate instead even very bulky linkers on substrates **1a−g**. At this point, the enantiodetermining C−C bond formation takes place, i.e., the attack of the *Si* face of the alkene to the activated alkyne, leading to cyclopropyl Au(I) carbene **III**.[52] Friedel−Crafts-type ring expansion, deprotonation of the Wheland intermediate, and protodeauration then afford species **IV**. Product/substrate ligand exchange is likely mediated by the anion[18b] via the intermediacy of species **I**, thus closing the cycle and releasing product **2**.

CONCLUSIONS

We describe the concept of asymmetric H-bonded counterion-directed catalysis, based on H-bonding interactions between a chiral anion and a suitably positioned H-bond donor group on JohnPhos-type ligands for Au(I). The presence of such interactions was substantiated by ^{1}H NMR titrations and structure−activity studies with modified ligands and chiral salts, as well as by the observed solvent and fluoride effects. For the first time, a broad range of alkyne substrates was engaged in challenging enantioselective gold-catalyzed reactions using chiral anions as the source of the stereochemical information, at catalyst loading down to 1 mol % and with excellent functional group tolerance.

This new paradigm, with a modular, short, and tunable synthesis of the two catalytic components, has the potential to speed up the development of enantioselective versions of various transition-metal catalyzed reactions, provided that the ligand for the metal of choice is equipped with a suitably placed H-bond donor group for a chiral anion.

ASSOCIATED CONTENT

Supporting Information

The Supporting Information is available free of charge at https://pubs.acs.org/doi/10.1021/jacs.1c11978.

Optimization tables, procedures, characterization, kinetic data, NMR spectra, SFC and HPLC traces, DFT computations, crystallographic data (PDF)

Accession Codes

CCDC 2107746−2107758 contain the supplementary crystallographic data for this paper. These data can be obtained free of charge via www.ccdc.cam.ac.uk/data_request/cif, or by emailing data_request@ccdc.cam.ac.uk, or by contacting The Cambridge Crystallographic Data Centre, 12 Union Road, Cambridge CB2 1EZ, UK; fax: +44 1223 336033.

AUTHOR INFORMATION

Corresponding Author

Antonio M. Echavarren − *Institute of Chemical Research of Catalonia (ICIQ), Barcelona Institute of Science and Technology, 43007 Tarragona, Spain; Departament de Química Orgànica i Analítica, Universitat Rovira i Virgili, 43007 Tarragona, Spain;* orcid.org/0000-0001-6808-3007; Email: aechavarren@iciq.es

Authors

Allegra Franchino − *Institute of Chemical Research of Catalonia (ICIQ), Barcelona Institute of Science and Technology, 43007 Tarragona, Spain*

Àlex Martí − *Institute of Chemical Research of Catalonia (ICIQ), Barcelona Institute of Science and Technology, 43007 Tarragona, Spain; Departament de Química Orgànica i Analítica, Universitat Rovira i Virgili, 43007 Tarragona, Spain*

Complete contact information is available at: https://pubs.acs.org/10.1021/jacs.1c11978

Notes

The authors declare no competing financial interest.

ACKNOWLEDGMENTS

We thank the MCIN/AEI/10.13039/501100011033 (Grants PID2019-104815GB-I00 and CEX2019-000925-S), the European Union (Horizon 2020 Marie Skłodowska-Curie COFUND Postdoctoral Fellowship 754510 to A.F.), the European Research Council (Advanced Grant 835080), the AGAUR (Grant 2017 SGR 1257 and FI Fellowship to À.M.), and CERCA Program/Generalitat de Catalunya for financial support. We also sincerely thank the ICIQ X-ray diffraction (especially Dr. Eduardo Escudero), NMR, chromatography, and mass spectrometry units.

REFERENCES

(1) Hamilton, G. L.; Kang, E. J.; Mba, M.; Toste, F. D. A Powerful Chiral Counterion Strategy for Asymmetric Transition Metal Catalysis. *Science* **2007**, *317*, 496−499.

(2) (a) Mayer, S.; List, B. Asymmetric Counteranion-Directed Catalysis. *Angew. Chem. Int. Ed.* **2006**, *45*, 4193−4195. (b) Mukherjee, S.; List, B. Chiral Counteranions in Asymmetric Transition-Metal Catalysis: Highly Enantioselective Pd/Brønsted Acid-Catalyzed Direct α-Allylation of Aldehydes. *J. Am. Chem. Soc.* **2007**, *129*, 11336−11337. (c) Phipps, R. J.; Hamilton, G. L.; Toste, F. D. The Progression of Chiral Anions from Concepts to Applications in Asymmetric Catalysis. *Nat. Chem.* **2012**, *4*, 603−614. (d) Mahlau, M.; List, B. Asymmetric Counteranion-Directed Catalysis: Concept, Definition, and Applications. *Angew. Chem., Int. Ed.* **2013**, *52*, 518−533. (e) Brak, K.; Jacobsen, E. N. Asymmetric Ion-Pairing Catalysis. *Angew. Chem., Int. Ed.* **2013**, *52*, 534−561. (f) Shirakawa, S.; Maruoka, K. Recent Developments in Asymmetric Phase-Transfer Reactions. *Angew. Chem., Int. Ed.* **2013**, *52*, 4312−4348.

(3) For work on the combination of achiral Au(I) complexes and chiral anions, see the following: (a) Reference 1. (b) LaLonde, R. L.; Wang, Z. J.; Mba, M.; Lackner, A. D.; Toste, F. D. Gold(I)-Catalyzed Enantioselective Synthesis of Pyrazolidines, Isoxazolidines, and Tetrahydrooxazines. *Angew. Chem., Int. Ed.* **2010**, *49*, 598−601. (c) Zi, W.; Toste, F. D. Gold(I)-Catalyzed Enantioselective Desymmetrization of 1,3-Diols through Intramolecular Hydroalkoxylation of Allenes. *Angew. Chem., Int. Ed.* **2015**, *54*, 14447−14451. (d) Pedrazzani, R.; An, J.; Monari, M.; Bandini, M. New Chiral BINOL-Based Phosphates for Enantioselective [Au(I)]-Catalyzed

Dearomatization of β-Naphthols with Allenamides. *Eur. J. Org. Chem.* **2021**, *2021*, 1732−1736.

(4) For work on the combination of chiral Au(I) complexes and chiral anions, see the following: (a) Aikawa, K.; Kojima, M.; Mikami, K. Axial Chirality Control of Gold(biphep) Complexes by Chiral Anions: Application to Asymmetric Catalysis. *Angew. Chem., Int. Ed.* **2009**, *48*, 6073−6077. (b) Aikawa, K.; Kojima, M.; Mikami, K. Synergistic Effect: Hydroalkoxylation of Allenes through Combination of Enantiopure BIPHEP-Gold Complexes and Chiral Anions. *Adv. Synth. Catal.* **2010**, *352*, 3131−3135. Corrigendum: Aikawa, K.; Kojima, M.; Mikami, K. *Adv. Synth. Catal.* **2011**, *353*, 2882−2883. (c) Barreiro, E. M.; Broggini, D. F. D.; Adrio, L. A.; White, A. J. P.; Schwenk, R.; Togni, A.; Hii, K. K. Gold(I) Complexes of Conformationally Constricted Chiral Ferrocenyl Phosphines. *Organometallics* **2012**, *31*, 3745−3754. (d) Miles, D. H.; Veguillas, M.; Toste, F. D. Gold(I)-Catalyzed Enantioselective Bromocyclization Reactions of Allenes. *Chem. Sci.* **2013**, *4*, 3427−3431. (e) Handa, S.; Lippincott, D. J.; Aue, D. H.; Lipshutz, B. H. Asymmetric Gold-Catalyzed Lactonizations in Water at Room Temperature. *Angew. Chem., Int. Ed.* **2014**, *53*, 10658−10662.

(5) (a) Mourad, A. K.; Leutzow, J.; Czekelius, C. Anion-Induced Enantioselective Cyclization of Diynamides to Pyrrolidines Catalyzed by Cationic Gold Complexes. *Angew. Chem., Int. Ed.* **2012**, *51*, 11149−11152. (b) Spittler, M.; Lutsenko, K.; Czekelius, C. Total Synthesis of (+)-Mesembrine Applying Asymmetric Gold Catalysis. *J. Org. Chem.* **2016**, *81*, 6100−6105.

(6) For a review on the combination of Au(I) methyl complexes and excess Brønsted acid for tandem reactions, see the following: (a) Inamdar, S. M.; Konala, A.; Patil, N. T. When gold meets chiral Brønsted acid catalysis: extending the boundaries of enantioselective gold catalysis. *Chem. Commun.* **2014**, *50*, 15124−15135. For selected examples, see the following: (b) Han, Z.-Y.; Xiao, H.; Chen, X.-H.; Gong, L.-Z. Consecutive Intramolecular Hydroamination/Asymmetric Transfer Hydrogenation under Relay Catalysis of an Achiral Gold Complex/Chiral Brønsted Acid Binary System. *J. Am. Chem. Soc.* **2009**, *131*, 9182−9183. (c) Muratore, M. E.; Holloway, C. A.; Pilling, A. W.; Storer, R. I.; Trevitt, G.; Dixon, D. J. Enantioselective Brønsted Acid-Catalyzed *N*-Acyliminium Cyclization Cascades. *J. Am. Chem. Soc.* **2009**, *131*, 10796−10797. (d) Liu, X.-Y.; Che, C.-M. Highly Enantioselective Synthesis of Chiral Secondary Amines by Gold(I)/Chiral Brønsted Acid Catalyzed Tandem Intermolecular Hydroamination and Transfer Hydrogenation Reactions. *Org. Lett.* **2009**, *11*, 4204−4207. (e) Tu, X.-F.; Gong, L.-Z. Highly Enantioselective Transfer Hydrogenation of Quinolines Catalyzed by Gold Phosphates: Achiral Ligand Tuning and Chiral-Anion Control of Stereoselectivity. *Angew. Chem., Int. Ed.* **2012**, *51*, 11346−11349. (f) Cala, L.; Mendoza, A.; Fañanás, F. J.; Rodríguez, F. A Catalytic Multicomponent Coupling Reaction for the Enantioselective Synthesis of Spiroacetals. *Chem. Commun.* **2013**, *49*, 2715−2717. (g) Zhou, S.; Li, Y.; Liu, X.; Hu, W.; Ke, Z.; Xu, X. Enantioselective Oxidative Multi-Functionalization of Terminal Alkynes with Nitrones and Alcohols for Expeditious Assembly of Chiral α-Alkoxy-β-aminoketones. *J. Am. Chem. Soc.* **2021**, *143*, 14703−14711.

(7) (a) Dorel, R.; Echavarren, A. M. Gold(I)-Catalyzed Activation of Alkynes for the Construction of Molecular Complexity. *Chem. Rev.* **2015**, *115*, 9028−9072. (b) Zuccarello, G.; Escofet, I.; Caniparoli, U.; Echavarren, A. M. New-Generation Ligand Design for the Gold Catalyzed Asymmetric Activation of Alkynes. *ChemPlusChem* **2021**, *86*, 1283−1296. (c) Barbazanges, M.; Augé, M.; Moussa, J.; Amouri, H.; Aubert, C.; Desmarets, C.; Fensterbank, L.; Gandon, V.; Malacria, M.; Ollivier, C. Enantioselective Ir^{I}-Catalyzed Carbocyclization of 1,6-Enynes by the Chiral Counterion Strategy. *Chem.—Eur. J.* **2011**, *17*, 13789−13794.

(8) Raducan, M.; Moreno, M.; Bour, C.; Echavarren, A. M. Phosphate Ligands in the Gold(I)-Catalysed Activation of Enynes. *Chem. Commun.* **2012**, *48*, 52−54.

(9) For reviews, see the following: (a) Jia, M.; Bandini, M. Counterion Effects in Homogeneous Gold Catalysis. *ACS Catal.* **2015**, *5*, 1638−1652. (b) Zuccaccia, D.; Del Zotto, A.; Baratta, W. The Pivotal Role of the Counterion in Gold Catalyzed Hydration and Alkoxylation of Alkynes. *Coord. Chem. Rev.* **2019**, *396*, 103−116. (c) Lu, Z.; Li, T.; Mudshinge, S. R.; Xu, B.; Hammond, G. B. Optimization of Catalysts and Conditions in Gold(I) Catalysis—Counterion and Additive Effects. *Chem. Rev.* **2021**, *121*, 8452−8477.

(10) For selected articles, see the following: (a) Zuccaccia, D.; Belpassi, L.; Tarantelli, F.; Macchioni, A. Ion Pairing in Cationic Olefin-Gold(I) Complexes. *J. Am. Chem. Soc.* **2009**, *131*, 3170−3171. (b) Zuccaccia, D.; Belpassi, L.; Rocchigiani, L.; Tarantelli, F.; Macchioni, A. A Phosphine Gold(I) π-Alkyne Complex: Tuning the Metal-Alkyne Bond Character and Counterion Position by the Choice of the Ancillary Ligand. *Inorg. Chem.* **2010**, *49*, 3080−3082. (c) Bandini, M.; Bottoni, A.; Chiarucci, M.; Cera, G.; Miscione, G. P. Mechanistic Insights into Enantioselective Gold-Catalyzed Allylation of Indoles with Alcohols: The Counterion Effect. *J. Am. Chem. Soc.* **2012**, *134*, 20690−20700. (d) Zhdanko, A.; Maier, M. E. Explanation of Counterion Effects in Gold(I)-Catalyzed Hydroalkoxylation of Alkynes. *ACS Catal.* **2014**, *4*, 2770−2775. (e) Biasiolo, L.; Del Zotto, A.; Zuccaccia, D. Toward Optimizing the Performance of Homogeneous L-Au-X Catalysts through Appropriate Matching of the Ligand (L) and Counterion (X^-). *Organometallics* **2015**, *34*, 1759−1765. (f) Lu, Z.; Han, J.; Okoromoba, O. E.; Shimizu, N.; Amii, H.; Tormena, C. F.; Hammond, G. B.; Xu, B. Predicting Counterion Effects Using a Gold Affinity Index and a Hydrogen Bonding Basicity Index. *Org. Lett.* **2017**, *19*, 5848−5851. (g) Schießl, J.; Schulmeister, J.; Doppiu, A.; Wörner, E.; Rudolph, M.; Karch, R.; Hashmi, A. S. K. An Industrial Perspective on Counter Anions in Gold Catalysis: Underestimated with Respect to "Ligand Effects". *Adv. Synth. Catal.* **2018**, *360*, 2493−2502.

(11) (a) Neel, A. J.; Hilton, M. J.; Sigman, M. S.; Toste, F. D. Exploiting Non-covalent π Interactions for Catalyst Design. *Nature* **2017**, *543*, 637−646. (b) Fanourakis, A.; Docherty, P. J.; Chuentragool, P.; Phipps, R. J. Recent Developments in Enantioselective Transition Metal Catalysis Featuring Attractive Noncovalent Interactions between Ligand and Substrate. *ACS Catal.* **2020**, *10*, 10672−10714.

(12) (a) Duarte, F.; Paton, R. S. Molecular Recognition in Asymmetric Counteranion Catalysis: Understanding Chiral Phosphate-Mediated Desymmetrization. *J. Am. Chem. Soc.* **2017**, *139*, 8886−8896. (b) Orlandi, M.; Coelho, J. A. S.; Hilton, M. J.; Toste, F. D.; Sigman, M. S. Parametrization of Non-covalent Interactions for Transition State Interrogation Applied to Asymmetric Catalysis. *J. Am. Chem. Soc.* **2017**, *139*, 6803−6806. (c) Shoja, A.; Reid, J. P. Computational Insights into Privileged Stereocontrolling Interactions Involving Chiral Phosphates and Iminium Intermediates. *J. Am. Chem. Soc.* **2021**, *143*, 7209−7215.

(13) Zhang, Z.; Smal, V.; Retailleau, P.; Voituriez, A.; Frison, G.; Marinetti, A.; Guinchard, X. Tethered Counterion-Directed Catalysis: Merging the Chiral Ion-Pairing and Bifunctional Ligand Strategies in Enantioselective Gold(I) Catalysis. *J. Am. Chem. Soc.* **2020**, *142*, 3797−3805.

(14) Michelet, V. Noble Metal-Catalyzed Enyne Cycloisomerizations and Related Reactions. *Comprehensive Organic Synthesis*, 2nd ed.; Elsevier, 2014; Vol. *5*, pp 1483−1536.

(15) For recent reviews on asymmetric gold catalysis, see the following: (a) Zi, W.; Toste, F. D. Recent Advances in Enantioselective Gold Catalysis. *Chem. Soc. Rev.* **2016**, *45*, 4567−4589. (b) Li, Y.; Li, W.; Zhang, J. Gold-Catalyzed Enantioselective Annulations. *Chem.—Eur. J.* **2017**, *23*, 467−512. (c) Jiang, J.-J.; Wong, M.-K. Recent Advances in the Development of Chiral Gold Complexes for Catalytic Asymmetric Catalysis. *Chem.—Asian J.* **2021**, *16*, 364−377. (d) Porcel García, S. Gold Catalyzed Asymmetric Transformations. IntechOpen, 2021; DOI: 10.5772/intechopen.97519. (e) Reference 7b.

(16) (a) Cheng, X.; Zhang, L. Designed Bifunctional Ligands in Cooperative Homogeneous Gold Catalysis. *CCS Chem.* **2021**, *3*, 1989−2002. (b) Zuccarello, G.; Zanini, M.; Echavarren, A. M. Buchwald-Type Ligands on Gold(I) Catalysis. *Isr. J. Chem.* **2020**, *60*, 360−372.

(17) (a) Schreiner, P. R. Metal-Free Organocatalysis through Explicit Hydrogen Bonding Interactions. *Chem. Soc. Rev.* **2003**, *32*, 289−296. (b) Doyle, A. G.; Jacobsen, E. N. Small-Molecule H-Bond Donors in Asymmetric Catalysis. *Chem. Rev.* **2007**, *107*, 5713−5743.
(18) For the only previous examples of phosphino(thio)urea Au(I) complexes, see the following: (a) Campbell, M. J.; Toste, F. D. Enantioselective Synthesis of Cyclic Carbamimidates via a Three-Component Reaction of Imines, Terminal Alkynes, and *p*-Toluenesulfonylisocyanate Using a Monophosphine Gold(I) Catalyst. *Chem. Sci.* **2011**, *2*, 1369−1378. (b) Franchino, A.; Martí, A.; Nejrotti, S.; Echavarren, A. M. Silver-Free Au(I) Catalysis Enabled by Bifunctional Urea- and Squaramide-Phosphine Ligands via H-Bonding. *Chem.—Eur. J.* **2021**, *27*, 11989−11996.
(19) (a) Akiyama, T. Stronger Brønsted Acids. *Chem. Rev.* **2007**, *107*, 5744−5758. (b) Terada, M. Binaphthol-derived Phosphoric Acid as a Versatile Catalyst for Enantioselective Carbon-Carbon Bond Forming Reactions. *Chem. Commun.* **2008**, 4097−4112. (c) Akiyama, T.; Mori, K. Stronger Brønsted Acids: Recent Progress. *Chem. Rev.* **2015**, *115*, 9277−9306. (d) Parmar, D.; Sugiono, E.; Raja, S.; Rueping, M. Complete Field Guide to Asymmetric BINOL-Phosphate Derived Brønsted Acid and Metal Catalysis: History and Classification by Mode of Activation; Brønsted Acidity, Hydrogen Bonding, Ion Pairing, and Metal Phosphates. *Chem. Rev.* **2014**, *114*, 9047−9153. Correction: Parmar, D.; Sugiono, E.; Raja, S.; Rueping, M. *Chem. Rev.* **2017**, *117*, 10608−10620.
(20) Wang, Y.; Wang, Z.; Li, Y.; Wu, G.; Cao, Z.; Zhang, L. A General Ligand Design for Gold Catalysis Allowing Ligand-Directed anti-Nucleophilic Attack of Alkynes. *Nat. Commun.* **2014**, *5*, 3470.
(21) (a) Zhang, Z.; Schreiner, P. R. (Thio)urea Organocatalysis—What Can Be Learnt from Anion Recognition? *Chem. Soc. Rev.* **2009**, *38*, 1187−1198. (b) Amendola, V.; Fabbrizzi, L.; Mosca, L. Anion Recognition by Hydrogen Bonding: Urea-Based Receptors. *Chem. Soc. Rev.* **2010**, *39*, 3889−3915. (c) Bregović, V. B.; Basarić, N.; Mlinarić-Majerski, K. Anion Binding with Urea and Thiourea Derivatives. *Coord. Chem. Rev.* **2015**, *295*, 80−124.
(22) For reviews on supramolecular ligands for asymmetric metal catalysis, see the following: (a) Meeuwissen, J.; Reek, J. N. H. Supramolecular Catalysis Beyond Enzyme Mimics. *Nat. Chem.* **2010**, *2*, 615−621. (b) Carboni, S.; Gennari, C.; Pignataro, L.; Piarulli, U. Supramolecular Ligand-Ligand and Ligand-Substrate Interactions for Highly Selective Transition Metal Catalysis. *Dalton Trans.* **2011**, *40*, 4355−4373. (c) Bellini, R.; van der Vlugt, J. I.; Reek, J. N. H. Supramolecular Self-Assembled Ligands in Asymmetric Transition Metal Catalysis. *Isr. J. Chem.* **2012**, *52*, 613−629. (d) Raynal, M.; Ballester, P.; Vidal-Ferran, A.; van Leeuwen, P. W. N. M. Supramolecular Catalysis. Part 1: Non-Covalent Interactions as a Tool for Building and Modifying Homogeneous Catalysts. *Chem. Soc. Rev.* **2014**, *43*, 1660−1733. (e) Ohmatsu, K.; Ooi, T. Design of Supramolecular Chiral Ligands for Asymmetric Metal Catalysis. *Tetrahedron Lett.* **2015**, *56*, 2043−2048. (f) Trouvé, J.; Gramage-Doria, R. Beyond Hydrogen Bonding: Recent Trends of Outer Sphere Interactions in Transition Metal Catalysis. *Chem. Soc. Rev.* **2021**, *50*, 3565−3584. For a seminal example involving ion-pairing interactions between an achiral ligand and a chiral anion, see the following: (g) Ohmatsu, K.; Ito, M.; Kunieda, T.; Ooi, T. Ion-Paired Chiral Ligands for Asymmetric Palladium Catalysis. *Nat. Chem.* **2012**, *4*, 473−477.
(23) Murata, M.; Buchwald, S. L. A General and Efficient Method for the Palladium-Catalyzed Cross-Coupling of Thiols and Secondary Phosphines. *Tetrahedron* **2004**, *60*, 7397−7403.
(24) Luchini, G.; Ascough, D. M. H.; Alegre-Requena, J. V.; Gouverneur, V.; Paton, R. S. Data-Mining the Diaryl(thio)urea Conformational Landscape: Understanding the Contrasting Behavior of Ureas and Thioureas with Quantum Chemistry. *Tetrahedron* **2019**, *75*, 697−702.
(25) Nakashima, D.; Yamamoto, H. Design of Chiral *N*-Triflyl Phosphoramide as a Strong Chiral Brønsted Acid and Its Application to Asymmetric Diels-Alder Reaction. *J. Am. Chem. Soc.* **2006**, *128*, 9626−9627.
(26) (a) Nieto-Oberhuber, C.; López, S.; Echavarren, A. M. Intramolecular [4 + 2] Cycloadditions of 1,3-Enynes or Arylalkynes with Alkenes with Highly Reactive Cationic Phosphine Au(I) Complexes. *J. Am. Chem. Soc.* **2005**, *127*, 6178−6179. (b) Nieto-Oberhuber, C.; Pérez-Galán, P.; Herrero-Gómez, E.; Lauterbach, T.; Rodríguez, C.; López, S.; Bour, C.; Rosellón, A.; Cárdenas, D. J.; Echavarren, A. M. Gold(I)-Catalyzed Intramolecular [4 + 2] Cycloadditions of Arylalkynes or 1,3-Enynes with Alkenes: Scope and Mechanism. *J. Am. Chem. Soc.* **2008**, *130*, 269−279.
(27) Previous asymmetric versions, all based on chiral ligands for Au(I), lack either scope or high enantiocontrol: (a) Two examples only (44−99% yield, 92−93% ee): Chao, C.-M.; Vitale, M. R.; Toullec, P. Y.; Genêt, J.-P.; Michelet, V. Asymmetric Gold-Catalyzed Hydroarylation/Cyclization Reactions. *Chem.—Eur. J.* **2009**, *15*, 1319−1323. (b) One further example (86% yield, 16% ee): Pradal, A.; Chao, C.-M.; Vitale, M. R.; Toullec, P. Y.; Michelet, V. Asymmetric Au-Catalyzed Domino Cyclization/Nucleophile Addition Reactions of Enynes in the Presence of Water, Methanol and Electron-rich Aromatic Derivatives. *Tetrahedron* **2011**, *67*, 4371−4377. (c) Five examples (70−95% yield, 73−88% ee): Delpont, N.; Escofet, I.; Pérez-Galán, P.; Spiegl, D.; Raducan, M.; Bour, C.; Sinisi, R.; Echavarren, A. M. Modular Chiral Gold(I) Phosphite Complexes. *Catal. Sci. Technol.* **2013**, *3*, 3007−3012. (d) One example only (99% yield, 91% ee): Aillard, P.; Dova, D.; Magné, V.; Retailleau, P.; Cauteruccio, S.; Licandro, E.; Voituriez, A.; Marinetti, A. The Synthesis of Substituted Phosphathiahelicenes *via* Regioselective Bromination of a Preformed Helical Scaffold: A New Approach to Modular Ligands for Enantioselective Gold-Catalysis. *Chem. Commun.* **2016**, *52*, 10984−10987. (e) 17 examples (61−99% yield, 58−92% ee): Zuccarello, G.; Mayans, J. G.; Escofet, I.; Scharnagel, D.; Kirillova, M. S.; Pérez-Jimeno, A. H.; Calleja, P.; Boothe, J. R.; Echavarren, A. M. Enantioselective Folding of Enynes by Gold(I) Catalysts with a Remote C_2-Chiral Element. *J. Am. Chem. Soc.* **2019**, *141*, 11858−11863. (f) One example only (92% yield, 94% ee): Magné, V.; Sanogo, Y.; Demmer, C. S.; Retailleau, P.; Marinetti, A.; Guinchard, X.; Voituriez, A. Chiral Phosphathiahelicenes: Improved Synthetic Approach and Uses in Enantioselective Gold(I)-Catalyzed [2 + 2] Cycloadditions of *N*-Homoallenyl Tryptamines. *ACS Catal.* **2020**, *10*, 8141−8148.
(28) *N*-Triflyl phosphoric amide **D1** has a pK_a value 0.9 units lower than the corresponding phosphoric acid **TRIP-H** (4.2 vs 3.3, both values in DMSO at 25 °C): Christ, P.; Lindsay, A. G.; Vormittag, S. S.; Neudörfl, J.-M.; Berkessel, A.; O'Donoghue, A. C. pK_a Values of Chiral Brønsted Acid Catalysts: Phosphoric Acids/Amides, Sulfonyl/Sulfuryl Imides, and Perfluorinated TADDOLs (TEFDDOLs). *Chem.—Eur. J.* **2011**, *17*, 8524−8528.
(29) Raubenheimer, H. G.; Schmidbaur, H. Gold Chemistry Guided by the Isolobality Concept. *Organometallics* **2012**, *31*, 2507−2522.
(30) Reid, J. P.; Goodman, J. M. Goldilocks Catalysts: Computational Insights into the Role of the 3,3′ Substituents on the Selectivity of BINOL-Derived Phosphoric Acid Catalysts. *J. Am. Chem. Soc.* **2016**, *138*, 7910−7917.
(31) (a) Kepp, K. P. A Quantitative Scale of Oxophilicity and Thiophilicity. *Inorg. Chem.* **2016**, *55*, 9461−9470. (b) Izaga, A.; Herrera, R. P.; Gimeno, M. C. Gold(I)-Mediated Thiourea Organocatalyst Activation: A Synergic Effect for Asymmetric Catalysis. *ChemCatChem* **2017**, *9*, 1313−1321.
(32) Reichardt, C. Solvatochromic Dyes as Solvent Polarity Indicators. *Chem. Rev.* **1994**, *94*, 2319−2358.
(33) All gold complexes used so far for the enantioselective cyclization of O-tethered 1,6-enynes bear chiral ligands. For a complete overview, see the following: (a) Mato, M.; Franchino, A.; García-Morales, C.; Echavarren, A. M. Gold-Catalyzed Synthesis of Small Rings. *Chem. Rev.* **2021**, *121*, 8613−8684. For seminal examples, see the following: (b) Chao, C.-M.; Beltrami, D.; Toullec, P. Y.; Michelet, V. Asymmetric Au(I)-Catalyzed Synthesis of Bicyclo[4.1.0]heptene Derivatives *via* a Cycloisomerization Process of 1,6-Enynes. *Chem. Commun.* **2009**, 6988−6990. (c) Teller, H.; Corbet, M.; Mantilli, L.; Gopakumar, G.; Goddard, R.; Thiel, W.;

https://doi.org/10.1021/jacs.1c11978
J. Am. Chem. Soc. 2022, 144, 3497−3509

Fürstner, A. One-Point Binding Ligands for Asymmetric Gold Catalysis: Phosphoramidites with a TADDOL-Related but Acyclic Backbone. *J. Am. Chem. Soc.* **2012**, *134*, 15331−15342.
(34) Sanjuán, A. M.; Martínez, A.; García-García, P.; Fernández-Rodríguez, M. A.; Sanz, R. Gold(I)-catalyzed 6-*endo* hydroxycyclization of 7-substituted-1,6-enynes. *Beilstein J. Org. Chem.* **2013**, *9*, 2242−2249.
(35) See Supporting Information for discussion on other nucleophiles and reaction side products.
(36) (a) Pfeifer, L.; Engle, K. M.; Pidgeon, G. W.; Sparkes, H. A.; Thompson, A. L.; Brown, J. M.; Gouverneur, V. Hydrogen-Bonded Homoleptic Fluoride-Diarylurea Complexes: Structure, Reactivity, and Coordinating Power. *J. Am. Chem. Soc.* **2016**, *138*, 13314−13325. (b) Ibba, F.; Pupo, G.; Thompson, A. L.; Brown, J. M.; Claridge, T. D. W.; Gouverneur, V. Impact of Multiple Hydrogen Bonds with Fluoride on Catalysis: Insight from NMR Spectroscopy. *J. Am. Chem. Soc.* **2020**, *142*, 19731−19744.
(37) D'Abrosca, B.; Fiorentino, A.; Golino, A.; Monaco, P.; Oriano, P.; Pacifico, S. Carexanes: Prenyl Stilbenoid Derivatives from *Carex distachya*. *Tetrahedron Lett.* **2005**, *46*, 5269−5272.
(38) Martín-Torres, I.; Ogalla, G.; Yang, J.-M.; Rinaldi, A.; Echavarren, A. M. Enantioselective Alkoxycyclization of 1,6-Enynes with Gold(I)-Cavitands: Total Synthesis of Mafaicheenamine C. *Angew. Chem., Int. Ed.* **2021**, *60*, 9339−9344.
(39) Witham, C. A.; Mauleón, P.; Shapiro, N. D.; Sherry, B. D.; Toste, F. D. Gold(I)-Catalyzed Oxidative Rearrangements. *J. Am. Chem. Soc.* **2007**, *129*, 5838−5839.
(40) Wang, W.; Yang, J.; Wang, F.; Shi, M. Axially Chiral N-Heterocyclic Carbene Gold(I) Complex Catalyzed Asymmetric Cycloisomerization of 1,6-Enynes. *Organometallics* **2011**, *30*, 3859−3869.
(41) (a) Yao, T.; Zhang, X.; Larock, R. C. $AuCl_3$-Catalyzed Synthesis of Highly Substituted Furans from 2-(1-Alkynyl)-2-alken-1-ones. *J. Am. Chem. Soc.* **2004**, *126*, 11164−11165. (b) Rauniyar, V.; Wang, Z. J.; Burks, H. E.; Toste, F. D. Enantioselective Synthesis of Highly Substituted Furans by a Copper(II)-Catalyzed Cycloisomerization-Indole Addition Reaction. *J. Am. Chem. Soc.* **2011**, *133*, 8486−8489. (c) Force, G.; Ki, Y. L. T.; Isaac, K.; Retailleau, P.; Marinetti, A.; Betzer, J.-F. Paracyclophane-based Silver Phosphates as Catalysts for Enantioselective Cycloisomerization/Addition Reactions: Synthesis of Bicyclic Furans. *Adv. Synth. Catal.* **2018**, *360*, 3356−3366.
(42) $^{31}P\{^1H\}$ and $^{19}F\{^1H\}$ NMR spectra remained unchanged, confirming that the chloride was not scavenged. See Supporting Information for details.
(43) (a) Burés, J. A Simple Graphical Method to Determine the Order in Catalyst. *Angew. Chem., Int. Ed.* **2016**, *55*, 2028−2031. (b) Burés, J. Variable Time Normalization Analysis: General Graphical Elucidation of Reaction Orders from Concentration Profiles. *Angew. Chem., Int. Ed.* **2016**, *55*, 16084−16087. (c) Nielsen, C. D.-T.; Burés, J. Visual Kinetic Analysis. *Chem. Sci.* **2019**, *10*, 348−353.
(44) Briggs, G. E.; Haldane, J. B. S. A Note on the Kinetics of Enzyme Action. *Biochem. J.* **1925**, *19*, 338−339. Application of this model rests on a series of underlying assumptions, all satisfied in the present case (see Supporting Information).
(45) (a) Michaelis, L.; Menten, M. L. Die Kinetik der Invertinwirkung. *Biochem. Z.* **1913**, *49*, 333−369. (b) Johnson, K. A.; Goody, R. S. The Original Michaelis Constant: Translation of the 1913 Michaelis−Menten Paper. *Biochemistry* **2011**, *50*, 8264−8269.
(46) Blackmond, D. G. Reaction Progress Kinetic Analysis: A Powerful Methodology for Mechanistic Studies of Complex Catalytic Reactions. *Angew. Chem., Int. Ed.* **2005**, *44*, 4302−4320. Correction: Blackmond, D. G. *Angew. Chem., Int. Ed.* **2006**, *45*, 2162−2162.
(47) Franchino, A.; Montesinos-Magraner, M.; Echavarren, A. M. Silver-Free Catalysis with Gold(I) Chloride Complexes. *Bull. Chem. Soc. Jpn.* **2021**, *94*, 1099−1117.
(48) Lineweaver, H.; Burk, D. The Determination of Enzyme Dissociation Constants. *J. Am. Chem. Soc.* **1934**, *56*, 658−666.
(49) The uncertainty refers not to experimental variation but only to the mathematical error of the linear regression, as determined by Excel LINEST routine. If all data from time 0 to 10 h are used in the Lineawer−Burk plot, a K_M value of 63 ± 4 is obtained, leading to identical conclusions regarding the partial order in substrate (see Supporting Information).
(50) Burés, J. What is the Order of a Reaction? *Top. Catal.* **2017**, *60*, 631−633.
(51) Geometry optimizations were carried out using Gaussian 09 at the B3LYP-D3/6-31G(d,p) level of theory in toluene (SMD). Single point energy calculations were performed on the resulting structures employing B3LYP-D3/6-311+G(d,p)/SMD(toluene). See the Supporting Information for an overview of all computed structures. Refer to ref 12c for an excellent discussion of alternative computational methods (functionals, basis sets, solvent models) in the context of chiral phosphate−iminium ion pairs.
(52) This step is assumed to be enantiodetermining on the basis of previous DFT calculations for the same reactions (refs 26 and 27e).

NOTE ADDED AFTER ASAP PUBLICATION

This paper was published February 9, 2022. References 2a,b have been added and the paper was re-posted February 17, 2022.

https://doi.org/10.1021/jacs.1c11978
J. Am. Chem. Soc. 2022, 144, 3497−3509